Available online at www.sciencedirect.com
SCIENCE DIRECT
Tetrahedron
Tetrahedron 62 (2006) 8035–8044

Monosubstituted thermotropic ferrocenomesogens containing heterocyclic pyrazole

Wen-Cheng Shen,[a] Yueh-Ju Wang,[a] Kung-Lung Cheng,[b] Gene-Hsiang Lee[c] and Chung K. Lai[a,*]

[a]*Department of Chemistry and Center for Nano Science Technology, National Central University, Chung-Li 320, Taiwan, ROC*
[b]*Union Chemical Laboratories, Industrial Technology Research Institute, Hsinchu 300, Taiwan, ROC*
[c]*Instrumentation Center, National Taiwan University, Taipei 10660, Taiwan, ROC*

Received 28 February 2006; revised 19 May 2006; accepted 8 June 2006
Available online 3 July 2006

Abstract—The synthesis and mesomorphic properties of two series of ferrocenyl derivatives, 5-[4-(4-alkoxylbenzyloxy)phenyl]-3-(4-ferrocenylphenyl)-1*H*-pyrazoles **1a** and 3-[4-(4-ferrocenylbenzyloxy)phenyl]-5-(4-alkoxylphenyl)-1*H*-pyrazoles **1b** are reported. Compounds **1a** exhibited either nematic (N) or smectic A (SmA) phases, whereas compounds **1b** formed N/SmC or SmA/SmC phases depending on the terminal carbon length. The formation of SmC phases in compounds **1b** was attributed to better molecular interaction between layers since the ferrocenyl unit was remotely located one phenyl ring away from pyrazole core. In contrast, their precursors, ferrocenyl β-diketonates, were in fact non-mesogenic. A less bent shape formed by ferrocenyl pyrazoles than ferrocenyl β-diketones was believed to be responsible for the formation of observed mesophases. The crystal and molecular structure of 3-[4-(4-ferrocenylbenzyloxy)phenyl]-5-(4-hexyloxyphenyl)-1*H*-pyrazole (**1b**; n=6) was determined by means of X-ray structural analysis. It crystallizes in the triclinic space group p-1, with a=11.0725(5) Å, b=12.5514(5) Å, c=14.2085(6) Å, and Z=2. The molecular arrangement was quite consistent with the layer structure observed by powder X-ray diffractometer. The cyclic voltammogram measured for **1** and **2** (n=16) indicated that incorporation of pyrazole group hardly influenced the electrochemical behavior of the ferrocenyl moiety.

1. Introduction

An increasing number of novel ferrocenomesogens or metallomesogens[1–2] derived from a ferrocenyl core have been reported and investigated since the first ferrocenyl Schiff bases exhibiting a nematic mesophase were synthesized and characterized by Malthête and Billard[3] in 1976. Most mesogenic ferrocenes[4,5] are structurally classified as monosubstituted,[5] 1,1′- or 1,3-disubstituted[4d] compounds. The molecular shapes resulting from the ferrocenomesogens were grouped[5a] as L-, S-, U-, and T-shape depending on the substitution and/or the position. Among them monosubstituted derivatives constitute the majority, which were also reviewed by Imrie.[5a] A ferrocenyl group located in the terminal position often resulted in a mono-molecular L-shape. A large distance of ca. 3.3 Å between the two Cp rings led to an unfavorable *l*/*d* ratio, and these two Cp rings often weakened the molecular interaction between the layers. On the other hand, a better geometric anisotropy was obtained by increasing the overall molecular length. Therefore, monoferrocenomesogens often contained a minimum of three phenyl groups. In a few examples, an extended S-shape evidenced by X-ray crystal structure[6] generated by two interlocked molecules in neighboring layers was used to explain the improved mesomorphic behavior. Most monosubstituted ferrocenomesogens gave rise to N, SmA, and/or SmC phases. The N phase was favored and often observed due to the repulsive steric effects of the ferrocenyl core because the resulting L-shape[6] molecules exhibited a reduced ability of the molecules to pack in more regular layers. The first ferrocenyl Schiff base derivatives with a chiral center exhibiting a TGBA/blue[7] phase apart from SmC*, SmA, and N* phase transformations are also known. A new type of mesogenic fullerene–ferrocene dyads[8] was prepared in 2004, and these compounds were found to exhibit enantiotropic SmA and organize into a partial bilayer structure. However, examples exhibiting a columnar phase[9] are relatively limited. The formation of hexagonal columnar phases by use of H-bonding interactions was demonstrated in tetracatenar covalent and bis-ferrocene derivatives.

Although metallomesogenic/mesogenic β-diketonates as their precursors have long been noted, compounds[10] derived from purely β-diketonates or pyrazoles are limited. Examples of ionic columnar metallomesogens[11] formed by three-coordinated copper(I) complexes were previously reported by this group. Other examples of novel structures formed

* Corresponding author. Tel.: +886 03 4259207; fax: +886 03 4277972; e-mail: cklai@cc.ncu.edu.tw

0040–4020/$ - see front matter © 2006 Elsevier Ltd. All rights reserved.
doi:10.1016/j.tet.2006.06.028

by trigold(I) pyrazoles[12] exhibiting columnar phases were also reported by Serrano[13] and Kim.[14] In this investigation, we report the synthesis and mesomorphic properties of the mesogenic ferrocenyl-based pyrazoles.

2. Results and discussion

2.1. Synthesis and characterization

The pyrazole derivatives were similarly prepared according to the literatures[11,13b] with minor modifications. The synthetic pathways followed to generate compounds **1a** and **1b** are summarized in Schemes 1 and 2. Ethyl 4-ferrocenylbenzoate was prepared by the reaction of ferrocene, ethyl 4-aminobenzoate, and sodium nitrite with a yield of ca. 34–40%. The β-diketones, isolated as deep red solids, were prepared by the reaction of methyl acetophenones and ethyl 4-ferrocenylbenzoate in the presence of NaH and 1,2-dimethoxyethane or THF. The reaction of β-diketones and hydrazine monohydrate in refluxing THF/EtOH gave pyrazole as yellow-to-orange solids. The compounds were characterized by ^{1}H, ^{13}C NMR spectroscopy and elemental analysis. The ratio of different tautomers in β-diketonates was determined by ^{1}H NMR spectroscopy. Two singlets at ca. 6.75–6.95 and 16.9–17.2 ppm were assigned to the proton of –CH═C and the enol–OH group, and the integration of each singlet was different depending on the solvent. However, the total integration of the two peaks was equal to two protons. A very broad peak at ca. 10.0–10.7 ppm assigned to the –NH proton in the pyrazoles[13b] was not observed for compounds **1a** and **1b**.

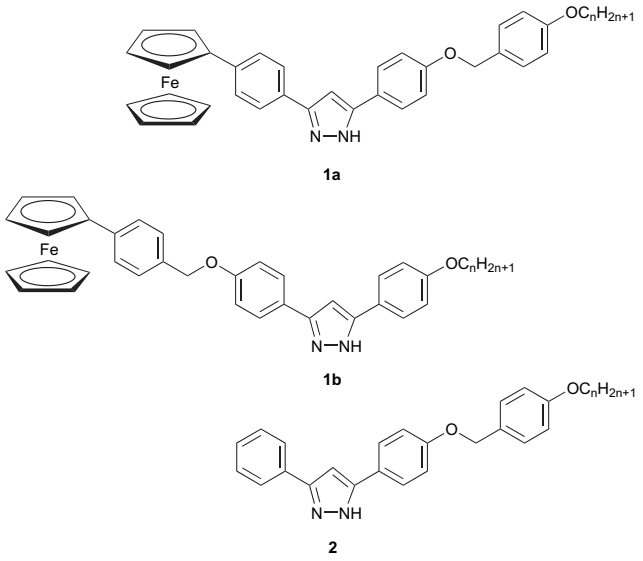

2.2. Single crystal structure 3-[4-(4-ferrocenylbenzyloxy)phenyl]-5-(4-hexyloxyphenyl)-1*H*-pyrazole (1b; *n*=6)

A single crystal grown from CH_2Cl_2/CH_3OH suitable for X-ray crystallography was obtained by diffusion technique.

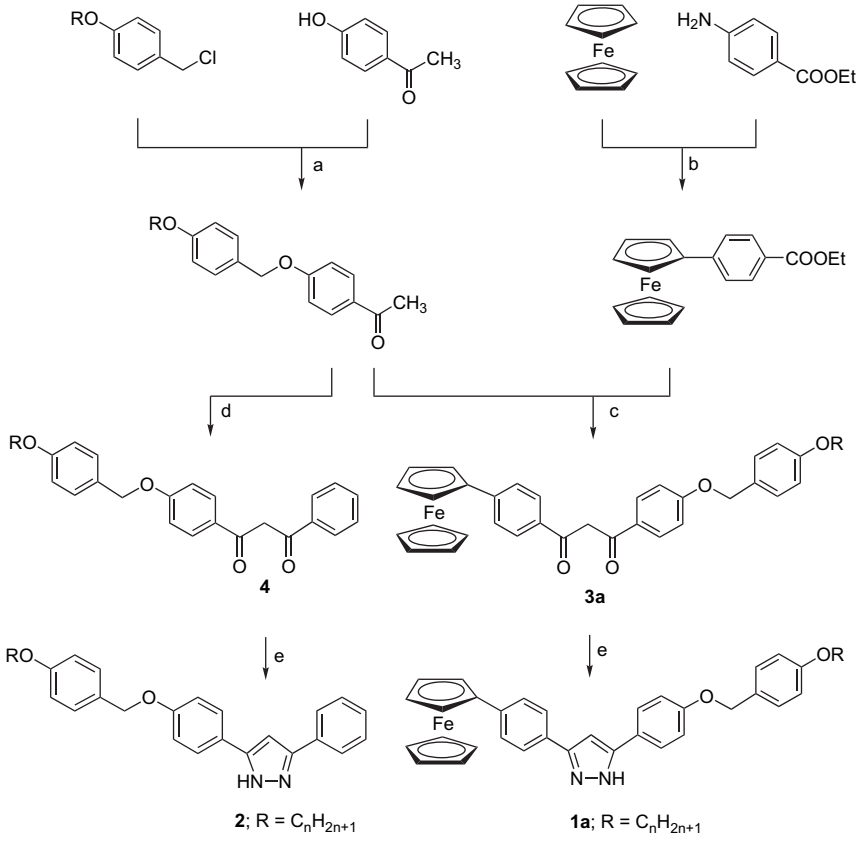

Scheme 1. Reagents and conditions: (a) K_2CO_3 (1.30 equiv), KI, refluxed in CH_3COCH_3, 48 h; (b) $NaNO_2$ (1.10 equiv), CH_3COONa (1.10 equiv), 10% H_2SO_4, stirred at 0 °C in CH_2Cl_2, 4 h; (c) NaH (6.0 equiv), refluxed in THF, 24 h; (d) methyl benzoate (1.0 equiv), NaH (6.0 equiv), refluxed in THF, 24 h; (e) $N_2H_4 \cdot H_2O$ (3.30 equiv), refluxed in dry THF/ethanol, 2 h.

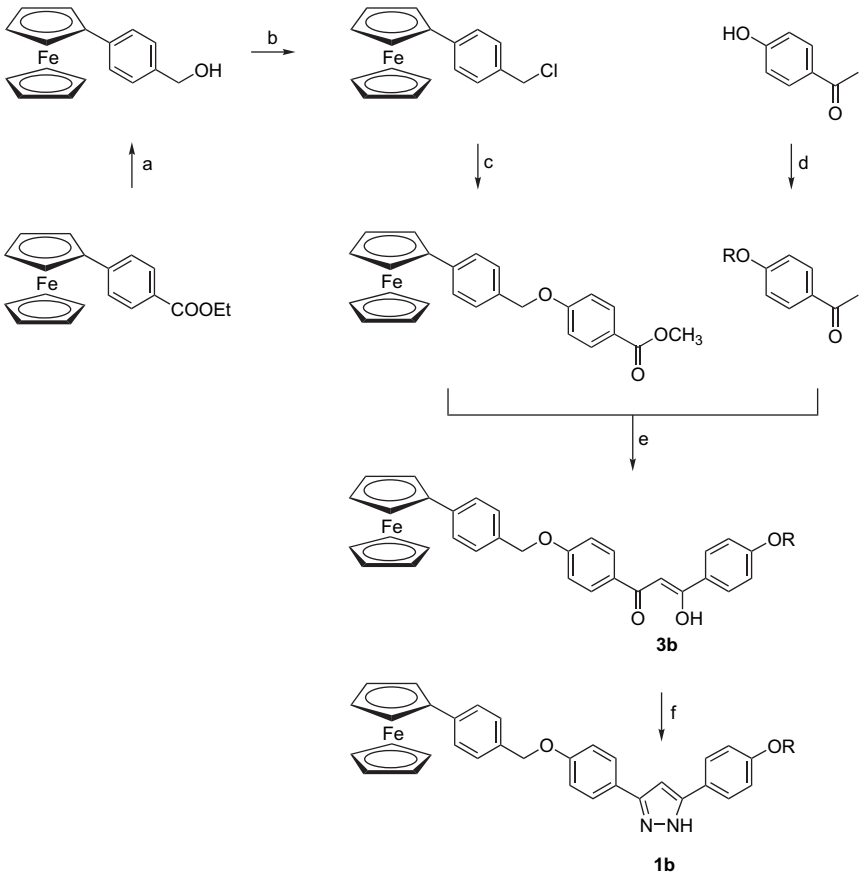

Scheme 2. Reagents and conditions: (a) $LiAlH_4$ (2.0 equiv), stirred at 0 °C in THF, then warmed up to rt, 24 h; (b) $SOCl_2$ (10.0 equiv), stirred in THF at rt, 4 h; (c) methyl 4-hydroxyacetophene (1.0 equiv), K_2CO_3 (1.30 equiv), KI, refluxed in CH_3COCH_3, 48 h; (d) RBr (1.0 equiv), K_2CO_3 (2.0 equiv), KI, refluxed in CH_3COCH_3, 48 h; (e) NaH (6.0 equiv), refluxed in THF, 24 h; (f) $N_2H_4 \cdot H_2O$ (3.30 equiv), refluxed in dry THF/absolute ethanol, 2 h.

Attempts to obtain a single crystal from CH_2Cl_2 were unsuccessful, which indicated that CH_3OH might play an important role in the crystal packing. The molecular structure with numbering scheme is shown in Figure 1. The unit cell is triclinic and the molecular geometry is fully extended and linear (Fig. 2). The overall molecular shape is described as elongated L-shape, and the molecular length measured ca. 29.10 Å. The two cyclopentadienyl rings were slightly staggered in conformation. Looking down from the top ring, the two cyclopentadienyl rings were rotated by ca. 10.63°–12.92°, which indicated that the conformation is between fully eclipsed and fully staggered. Three aromatic rings except for the second one from the Cp ring were in fact considered as parallel with the Cp ring. The torsion angles between the substituted cyclopentadienyl ring and the other four aromatic rings were calculated as ~2.39°, ~29.26°, ~0.41°, and ~8.05°, respectively. The torsion angle of the second phenyl ring with the pyrazole ring (C22–C21–C24–N1) was measured as ~31.67°. A view of the crystal packing in the unit cell is presented in Figure 2 and reveals that the molecules are packed in a parallel arrangement within the layers. The molecules were arranged parallel to each other in an extended fashion in a head-to-tail/tail-to-head format, and the closest distance between the two molecules was 2.605 Å, as shown in Figure 3. A CH–π stacking interaction (3.725 Å) within the layer was also possible. The distance of H-bonding interaction between N-atom on the pyrazole and the O-atom on the methanol was measured as 2.099 Å. This molecular arrangement was quite consistent with the layered structure observed by powder XRD.

2.3. Mesogenic properties

The phase behavior of these compounds was characterized and studied by differential scanning calorimetry (DSC) and polarized optical microscopy. The thermal behavior of

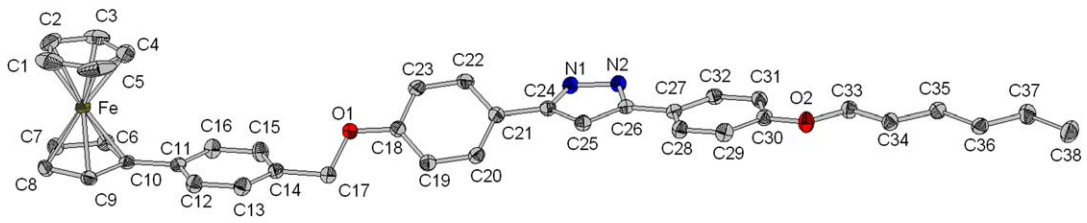

Figure 1. An ORTEP drawing for **1b** (n=6) with the numbering scheme. The thermal ellipsoids of the non-hydrogen atoms are drawn at the 50% probability level. It crystallizes in the triclinic space group P-1, with a=11.0725(5) Å, b=12.5514(5) Å, c=14.2085(6) Å, and Z=2.

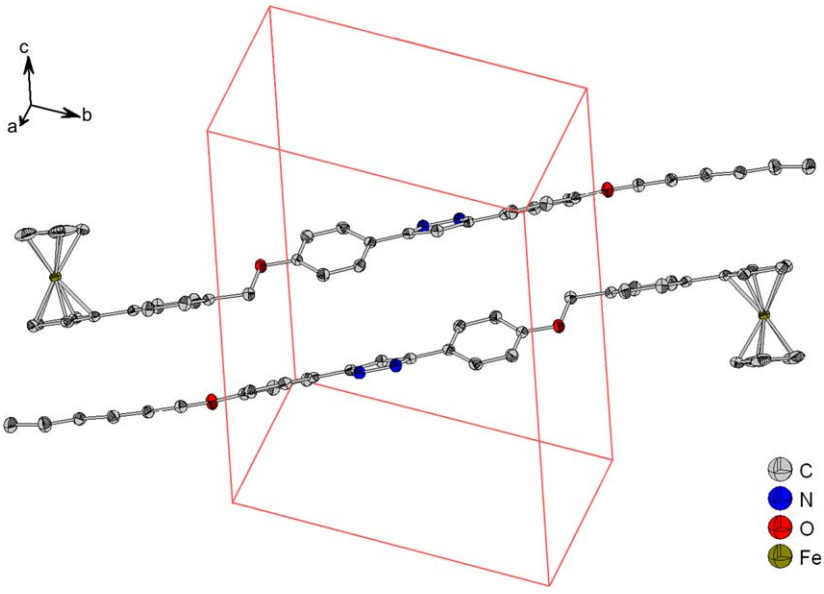

Figure 2. The crystal packing in the unit cell showing the two parallel molecules.

ferrocenyl pyrazoles **1a** and **1b** is summarized in Tables 1 and 2. All compounds **1a**–**1b** exhibited mesomorphic properties. Compounds **1a** with shorter alkyl chains exhibited a monotropic N phase (n=6, 8) or monotropic SmA phases (n=10), however, an enantiotropic SmA phase was observed for other compounds **1a** with longer terminal chains (n=12, 14, 16). The optical texture of N or SmA phase was observed by optical microscope (Fig. 4). The N phase exhibited Schlieren textures, whereas the SmA phase appeared as a focal-conic fan texture with a large area of homeotropic domains. The clearing temperatures were insensitive to the terminal chain length, and ranged between 182.2 and 188.7 °C. The insensitivity of the clearing temperatures to chain length indicated that the formation of the mesophase was not controlled and/or determined by the dispersive force of terminal chains. The temperature ranges of mesophases were quite narrow, ca. 8.0–13.9 °C on heating cycle or ca. 14.0–33.8 °C on cooling cycle. The enthalpies of I→N transition were relatively low in the values of 1.40–1.94 kJ/mol, and the enthalpies of I→SmA transition ranged from 3.87 to 5.22 kJ/mol. The narrow range of mesophase temperature indicated that the mesophase was not kinetically stable, which revealed the important role of the ferrocenyl core in the molecular packing. Ferrocenyl moiety as a relatively steric core led to the molecular packing ineffective. In contrast, all their precursor β-diketones were in fact non-mesogenic. The difference observed in the formation of mesophases formed by these two types of compounds was probably attributed to complementary molecular shapes required to be mesogenic. Pyrazoles are comparatively less bent shape

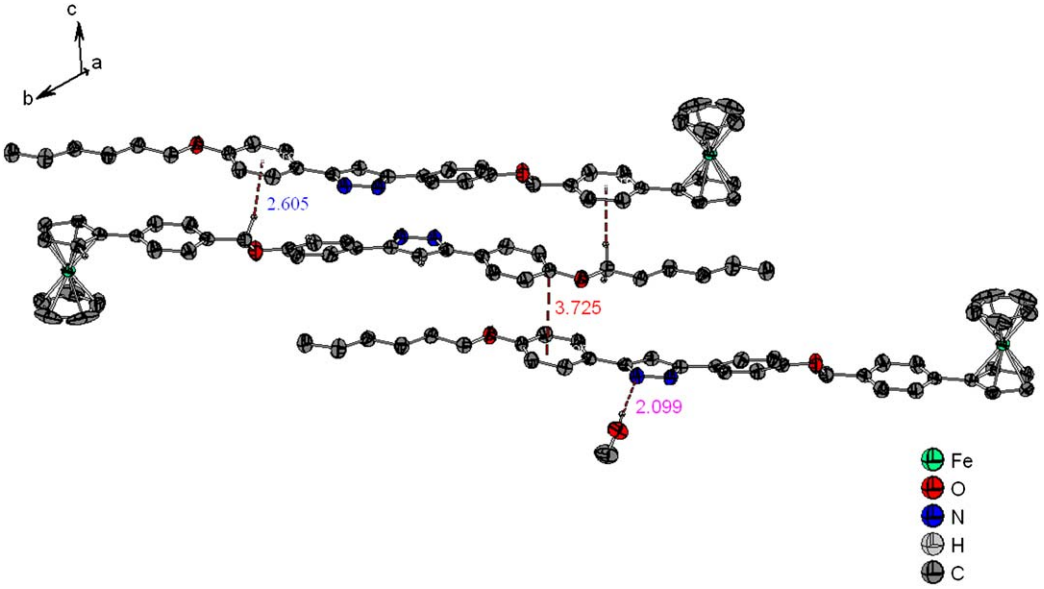

Figure 3. Some crystallographic data. (a) 2.605 Å; the π–CH interaction; (b) 3.725 Å; the π–π interaction; and (c) 2.099 Å; H-bond bonding between the O-atom on the CH_3OH and N-atom on the pyrazole ring.

Table 1. The phase transition temperatures and the enthalpies of compounds **1a** and **2**

1a; n = 6			Cr	162.5 (31.6)	186.2 (35.7)	N	179.2 (1.40)		Iso
8			Cr	163.7 (35.0)	188.7 (43.6)	N	177.7 (1.94)		Iso
10			Cr	156.9 (32.7)	182.2 (41.7)	SmA	178.1 (4.45)		Iso
12			Cr	151.3 (29.4)	175.2 (30.5)	SmA	183.2 (3.88)		Iso
14	Cr_1	143.2 (8.23) 146.6 (8.24)	Cr_2	150.7 (21.2)	173.1 (22.5)	SmA	184.5 (5.05)	187.0 (5.25)	Iso
16	Cr_1	140.7 (14.6) 146.0 (14.7)	Cr_2	151.1 (27.9)	171.7 (30.0)	SmA	182.0 (5.22)	183.2 (5.42)	Iso
2; n = 6			Cr	130.1 (18.2)	155.5 (18.4)	SmA	176.3 (5.15)	178.3 (5.29)	Iso
12			Cr	119.3 (27.5)	142.6 (27.7)	SmA	181.5 (6.47)	184.6 (7.13)	Iso
16			Cr	113.3 (29.3)	136.7 (29.5)	SmA	182.6 (7.71)	184.2 (7.58)	Iso

n represents the number of carbons in the alkoxy chain. K is crystal phase; SmA is smectic A phase; N is nematic phase; Iso is isotropic.

Table 2. The phase temperatures and enthalpies of compounds **1b** and **4**

1b; n = 6	Cr_1	113.2 (11.5) 114.9 (1.63)	Cr_2		SmC	173.7 (1.07) 195.7 (45.6)	N	192.2 (2.25) 197.0[a]	Iso		
8	Cr_1	117.3 (13.9) 158.5 (0.33)	Cr_2	176.6 (17.4)	SmC	176.3 (0.30) 191.7 (0.41)	N	186.6 (0.71) 193.0[a]	Iso		
10	Cr_1	111.9 (13.0) 133.2 (1.47)	Cr_2	175.0 (29.8)	SmC	178.8 (1.37) 188.3 (2.45)	N	186.9 (2.63) 192.0[a]	Iso		
12	Cr_1	68.4 (7.34)	Cr_2	120.4 (19.4) 168.5 (24.4)	SmC	174.1 (0.51) 181.1 (1.89)	N	180.6 (0.46) 188.0[a]	Iso		
14	Cr_1	69.6 (5.12)	Cr_2	114.3 (25.5) 168.0 (30.0)	SmC	169.1 (0.34) 183.1 (4.72)	SmA	180.5 (4.2) 186.0[a]	Iso		
16	Cr_1	68.8 (3.83) 82.5 (6.18)	Cr_2	112.8 (21.2) 168.2 (25.5)	SmC	166.7[a] 182.5 (4.45)	SmA	176.2 (3.24) 184.0[a]	Iso		
4; n = 10							Cr	76.2 (23.1) 140.5 (39.0)	Iso		
12							Cr	73.9 (21.7) 120.1 (38.5)	Iso		
14							Cr	80.9 (41.8) 122.4 (42.3)	Iso		

[a] Determined by optical microscope. SmC is smectic phase. Also see Table 1 for term definitions.

than their precursor β-deketones, required for the formation of calamitic mesogens.

To better understand the effect of steric ferrocenyl group on the formation of mesophases, compounds **2** without the ferrocenyl moiety incorporated were also prepared and their mesomorphic properties were studied. The thermal behavior of compounds **2** (n=6, 12, 16) is listed in Table 1. The effect of incorporating ferrocenyl moieties is very marked. Instead of the monotropic behavior observed in compounds **1a** (n=6, 8), all compounds **2** (n=6, 12, 16) formed enantiotropic phases. SmA phases (see Fig. 5) were all observed. The clearing temperatures ranged from ca. 178.3 to 184.6 °C, similar to those in compounds **1a** containing the

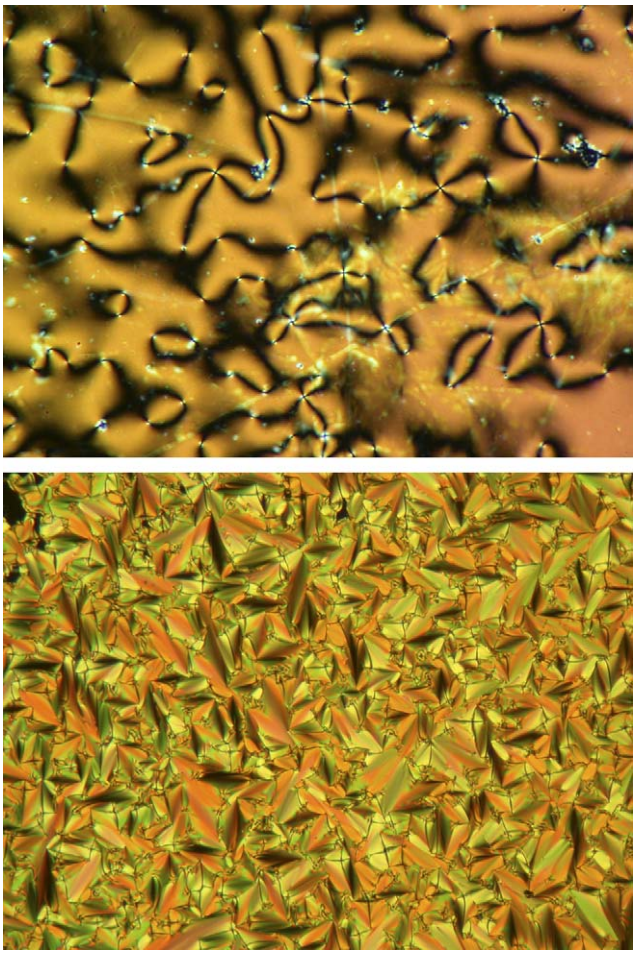

Figure 4. Optical textures of N phase at 174 °C (top plate) observed by **1a** (n=8) and SmA phase at 110 °C (bottom plate) observed by **1a** (n=12).

same carbon chain length. The clearing temperature was shown to be less influenced by the presence of a steric ferrocenyl group. However, the temperature range of SmA phases observed on cooling cycle was measured at ca. 46.2–69.3 °C, which was relatively much wider than that for compounds **1a**. In contrast, the range of mesophase temperatures increased with the carbon chain length (ΔT=46.2 °C, 62.2 °C, and 69.3 °C for n=6, 12, and 16). The mesophase formed by compounds **2** is apparently more kinetically stable than that by compounds **1a**. Therefore, the results indicated that the steric ferrocenyl unit played an important role in the formation of mesophase in this type of ferrocenyl pyrazole.

Variable temperature powder XRD diffractometer was used to confirm the structure of the mesophases. A diffraction pattern for compounds **1a** (n=16) at 178 °C is given in Figure 6, which was characteristic of the SmA phase. The d-spacing of 36.73 Å corresponded to the layer distance, and was close to 34.25 Å, the molecular length estimated for compound **1a**.

In order to improve the mesophase, we also prepared a series of compounds **1b**. Compounds **1b** were structurally similar to compounds **1a**, however, pyrazole ring in **1b** was one benzyl group further away from the –Cp group. The molecular length and molecular weight are identical in both **1a** and **1b**, however, the overall molecular length and/or shape

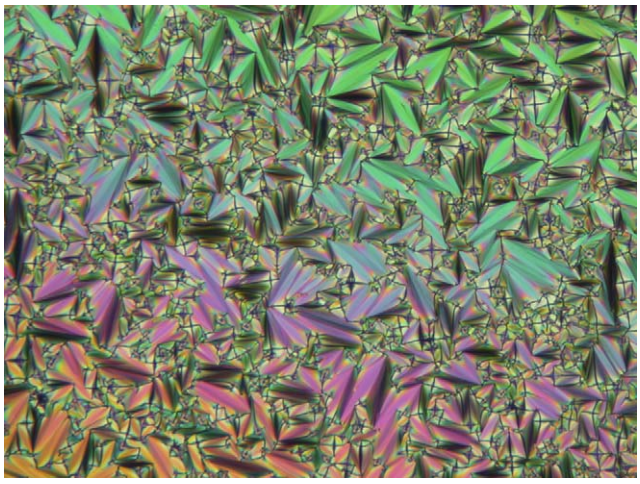

Figure 5. Optical texture of SmA phase at 167 °C observed by **2** (n=12).

formed by compounds **1a** and **1b** are slightly different due to their conformers. The thermal behavior of compounds **1b** is listed in Table 2. All mesogenic phases except for the SmC phase with n=6 were kinetically enantiotropic. Besides the N or SmA phase observed in compounds **1a**, an extra smectic C phase was observed in the entire series. Compounds with a shorter terminal carbon chain (n=6, 8, 10, 12) formed N and SmC phases, however, compounds with a longer carbon chain (n=14, 16) formed SmA and SmC phases. The clearing temperatures slightly decreased with carbon chain length. Some of transition temperatures were directly obtained by optical microscopy (see Fig. 7) due to their relatively small enthalpies of phase transitions. They were all ranged from 197.0 (n=6) to 184.0 °C (n=16). However, the temperature ranges of mesophases measured at ca. 60.2–79.0 °C on cooling cycle were much wider (i.e., 14.0–33.8 °C) than those in compounds **1a**. In addition, the observation of SmC phases in compounds **1b** was probably attributed to the better molecular attraction between the layers than in compounds **1a**. On the other hand, their precursors, β-diketones **4**, were also non-mesogenic, and only transitions of crystal-to-isotropic at 140.5 °C

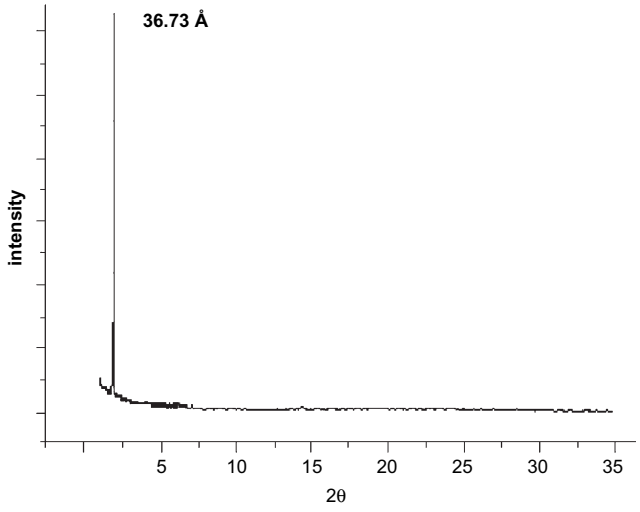

Figure 6. X-ray diffraction pattern of compound **1a** (n=16) at 178.0 °C.

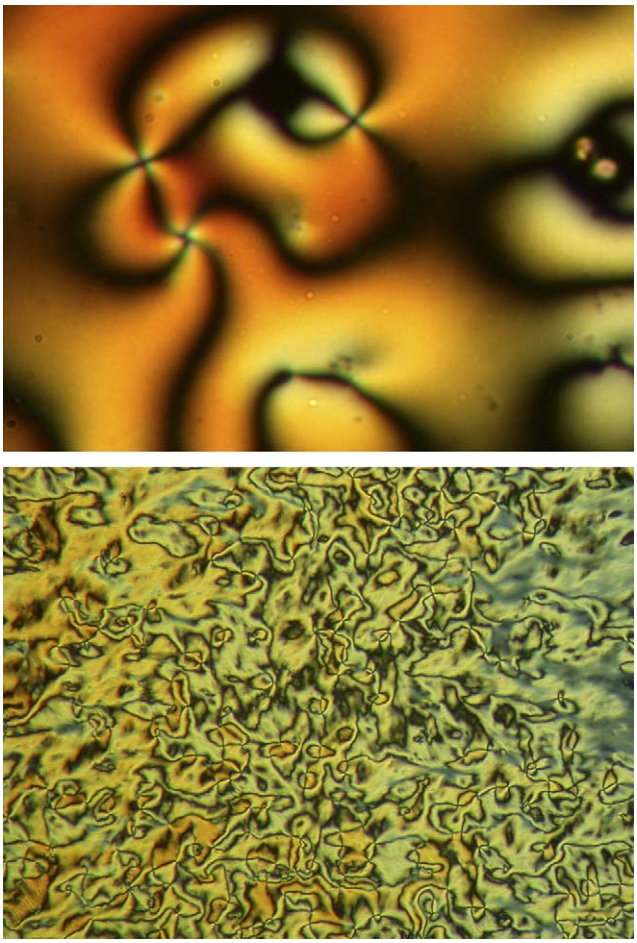

Figure 7. Optical textures of N phase at 179 °C (top) and SmC phase at 159 °C observed by **1b** (n=12).

(n=10), 120.1 °C (n=12), and 122.4 °C (n=14) were observed (Table 2).

The electrochemical behavior of two compounds **1** (n=16) and **2** (n=16) was also investigated by cyclic voltammetry measured in CH_2Cl_2. The E_{ox} data measured with a scan rate of 100 mV/s are reported relative to ferrocene, which has an E_{ox} at 135 mV relative to Ag/Ag^+, and the anodic peak–cathodic peak separation (ΔE_p) is 80 mV. Compound **1** (n=16) has an E_{ox} at 15 mV and compound **2** (n=16) has an E_{ox} at 25 mV. The data indicate that both compounds **1** (ΔE_p=85) and **2** (ΔE_p=70) have one reversible redox process, which is similar to unsubstituted ferrocene.

3. Conclusion

Though the ferrocenyl moiety could be considered as a relatively bulky group, the mesomorphic behavior of two series of newly prepared monosubstituted ferrocenomesogens was improved by structural modification. A small mesogenic domain due to the unfavorable packing caused by the relatively large ferrocenyl group can be reduced or minimized by increasing the overall molecular length. However, a less bent structure deviated significantly from better linearity compared with their precursors, diketonates, was used to explain the lack of mesogenic behavior.

4. Experimental

4.1. General procedures

All chemicals and solvents were reagent grade from Lancaster or Aldrich. Solvents were dried by standard techniques. ^1H and ^{13}C NMR spectra were measured on a Bruker AM-300. FTIR spectra were performed on Nicolet Magna-IR 550 spectrometer. DSC thermographs were carried out on a Mettler DSC 821 and calibrated with a pure indium sample (mp 156.60 °C, 28.45 J/K), and all phase transitions were determined using a scan rate of 10.0 °C/min. Optical polarized microscopy was carried out on an Zeiss AxiaPlan equipped with a hot stage system of Mettler FP90/FP82HT. Elemental analysis for carbon, hydrogen, and nitrogen was conducted on a Heraeus Vario EL-III elemental analyzer at National Taiwan University. Methyl-4-alkoxylbenzoates,[15a] 4-alkoxybenzyl alcohols,[15b] 4-alkoxybenzyl chlorides,[15c] 4-alkoxyacetophenones,[15d] and 4-(4-alkoxybenzyloxy)-phenyl methyl ketone[15d] were prepared by literature procedures. Synthetic procedures and characterization data of selected compounds are presented in the following sections.

4.1.1. 4-(4-Hexadecyloxybenzyloxy)phenyl methyl ketone[15d] (n=16). White solid, yield 86%. ^1H NMR ($CDCl_3$): δ 0.86 (t, J=6.1 Hz, $-CH_3$, 3H), 1.25–1.81 (m, $-CH_2$, 28H), 2.53 (s, $-OCH_3$, 3H), 3.93 (t, J=6.5 Hz, $-OCH_2$, 2H), 5.03 (s, $-CH_2$, 2H), 6.90 (d, J=5.8 Hz, $-C_6H_4$, 2H), 6.98 (d, J=6.9 Hz, $-C_6H_4$, 2H), 7.32 (d, J=8.6 Hz, $-C_6H_4$, 2H), 7.91 (d, J=6.9 Hz, $-C_6H_4$, 2H). ^{13}C NMR ($CDCl_3$): δ 14.09, 22.68, 26.02, 29.21, 29.37, 29.59, 29.69, 31.92, 67.92, 69.86, 114.37, 114.41, 127.70, 129.15, 130.21, 130.42, 159.08, 162.58, 196.69.

4.1.2. Ethyl 4-ferrocenylbenzoate. Ethyl 4-ferrocenylbenzoate was similarly prepared by the diazonium methods.[5b,6c] The mixture of ethyl 4-aminobenzoate (2.00 g, 12 mmol) and powdered $NaNO_2$ (0.92 g, 13 mmol) was dissolved in 10 mL of distilled water, and the solution was stirred for 10 min. To the solution, dilute H_2SO_4 (10%, 10.0 mL) was dropwise added at ice bath temperature, and the mixture was stirred for 20 min. The solution was then filtered to remove insoluble solids, and the solution was kept at 0 °C. The solution of ferrocene (2.25 g, 12 mmol) dissolved in 10.0 mL of CH_2Cl_2 and the aqueous solution of CH_3COONa (0.78 g, in 10.0 mL H_2O) were simultaneously added dropwise in a two-neck flask, and the solution was stirred for 2 h. The deep blue solution was extracted three times with methylene chloride. The deep red organic layers were collected and dried with anhydrous $MgSO_4$. The product was purified by flash chromatography with eluting hexane/CH_2Cl_2 (5:1). Red crystals were isolated after recrystallization from hexane. Yield 38%. ^1H NMR ($CDCl_3$): δ 1.41 (t, J=2.4 Hz, $-CH_3$, 3H), 4.02 (s, $-C_5H_5$, 5H), 4.35 (m, $-C_5H_4$, $-OCH_2$, 4H), 4.69 (t, J=1.9 Hz, $-C_5H_4$, 2H), 7.48 (d, J=8.5 Hz, $-C_6H_4$, 2H), 7.97 (d, J=8.5 Hz, $-C_6H_2$, 2H). ^{13}C NMR ($CDCl_3$): δ 14.26, 60.65, 66.72, 69.61, 69.67, 83.22, 125.42, 127.49, 129.52, 144.83, 166.52.

4.1.3. 1-[4-(4-Hexadecyloxybenzyloxy)phenyl]-3-(4-ferrocenylphenyl)propane-1,3-dione (3a; n=16). A similar compound[16] has been prepared. A mixture of powder

NaH (1.08 g, 0.045 mol) and 4-hexadecyloxybenzylacetophenone (4.2 g, 0.009 mol) was dissolved in 50 mL of dried THF under nitrogen atmosphere. The solution was then added to the solution of ethyl 4-ferrocenylbenzoate (3.0 g, 0.009 mol) in 20 mL of THF, and the solution was refluxed for 24 h. The solution was carefully neutralized with 150 mL of dilute hydrochloric acid (1.0 M, 1.0 mL), and then extracted twice with 100 mL of CH_2CH_2/H_2O (1:1). The organic layers were combined and dried over anhydrous $MgSO_4$. The product, isolated as deep red solids, was obtained after recrystallization from CH_2Cl_2/MeOH. Yield 68%. ^{1}H NMR ($CDCl_3$): δ 0.84 (t, J=6.6 Hz, –CH_3, 3H), 1.24–1.80 (m, –CH_2, 28H), 3.97 (t, J=6.5 Hz, –OCH_2, 2H), 4.05 (s, C_5H_5, 5H), 4.38 (t, J=1.7 Hz, C_5H_4, 2H), 4.71 (t, J=1.8 Hz, C_5H_4, 2H), 5.05 (s, –CH_2, 2H), 6.78 (s, –CCHCO, 1H), 6.91 (d, J=8.6 Hz, C_6H_4, 2H), 7.03 (d, J=8.8 Hz, C_6H_4, 2H), 7.33 (d, J=8.5 Hz, C_6H_4, 2H), 7.53 (d, J=8.4 Hz, C_6H_4, 2H), 7.88 (d, J=8.4 Hz, C_6H_4, 2H), 7.96 (d, J=8.8 Hz, C_6H_4, 2H), 17.11 (s, –OH, 1H). ^{13}C NMR ($CDCl_3$): δ 13.99, 22.55, 25.88, 29.09, 29.22, 29.45, 29.54, 31.78, 66.69, 67.92, 69.69, 69.89, 83.27, 91.86, 114.50, 114.66, 125.74, 127.03, 127.78, 128.24, 129.06, 129.16, 132.59, 144.47, 159.09, 162.64, 183.86, 185.44. FABMS (m/z), calcd for M^+ 754.82, found 754.64. FTIR (KBr): 3099, 2921, 2852, 1605, 1518, 1252, 1229, 1173, 1038, 1011, 849, 813, 790 cm^{-1}. Anal. Calcd for $C_{48}H_{58}O_4Fe$: C, 76.38; H, 7.74. Found: C, 76.77; H, 7.93.

4.1.4. 5-[4-(4-Hexadecyloxybenzyloxy)phenyl]-3-(4-ferrocenylphenyl)-1*H*-pyrazole (1a; *n*=16). A hot solution of 1-[4-(4-hexadecyloxybenzyloxy)phenyl]-3-(4-ferrocenylphenyl)propane-1,3-dione (5.0 g, 6.7 mmol) dissolved in THF/EtOH (1:1) was slowly added to the solution of hydrazine monohydrate (1.06 mL, 22.0 mmol) under nitrogen atmosphere. The solution was gently refluxed for 2 h and then stirred at room temperature for 12 h. The solution was concentrated, and the product isolated as yellow solids was obtained after recrystallization from THF/hexane. Yield 80%. ^{1}H NMR ($CDCl_3$): δ 0.87 (t, J=6.2 Hz, –CH_3, 3H), 1.24–1.76 (m, –CH_2, 28H), 3.96 (t, J=6.5 Hz, –OCH_2, 2H), 4.04 (s, C_5H_5, 5H), 4.32 (t, J=1.7 Hz, C_5H_4, 2H), 4.67 (t, J=1.9 Hz, C_5H_4, 2H), 5.01 (s, –CH_2, 2H), 6.74 (s, –CCHCO, 1H), 6.88 (d, J=8.6 Hz, C_6H_4, 2H), 6.96 (d, J=8.8 Hz, C_6H_4, 2H), 7.33 (d, J=8.5 Hz, C_6H_4, 2H), 7.50 (d, J=8.3 Hz, C_6H_4, 2H), 7.62 (d, J=8.6 Hz, C_6H_4, 4H). ^{13}C NMR ($CDCl_3$): δ 13.95, 22.53, 25.86, 29.05, 29.22, 29.43, 29.52, 31.75, 66.40, 67.91, 68.82, 69.85, 84.81, 98.87, 114.44, 115.00, 126.15, 126.77, 127.59, 128.35, 129.11, 134.04, 139.10, 158.79, 158.93. FABMS (m/z), calcd for M^+ 750.83, found 750.79. FTIR (KBr): 3297, 3232, 3143, 3099, 3035, 2952, 2928, 2867, 2859, 1619, 1518, 1454, 1443, 1257, 1178, 840, 797 cm^{-1}. Anal. Calcd for $C_{48}H_{58}N_2O_2Fe$: C, 76.78; H, 7.79; N, 3.73. Found: C, 76.55; H, 7.91; N, 3.71.

4.1.5. 1-[4-(4-Dodecyloxybenzyloxy)phenyl]-3-phenylpropane-1,3-dione (4; *n*=12). White solid, yield 78%. ^{1}H NMR ($CDCl_3$): δ 0.88 (t, J=6.7 Hz, –CH_3, 3H), 1.24–1.80 (m, –CH_2, 20H), 3.95 (t, J=6.5 Hz, –OCH_2, 2H), 5.03 (s, –CH_2, 2H), 6.79 (s, –CCHCO, 1H), 6.91 (d, J=8.6 Hz, –C_6H_4, 2H), 7.03 (d, J=8.7 Hz, –C_6H_4, 2H), 7.33 (d, J=8.5 Hz, –C_6H_4, 2H), 7.44 (d, J=6.2 Hz, –C_6H_4, 2H), 7.52 (d, J=6.8 Hz, –C_6H_5, 2H), 7.57 (s, –C_6H_5, 1H), 7.96 (d, J=8.8 Hz, –C_6H_5, 2H), 17.10 (s, –OH, 1H). ^{13}C NMR ($CDCl_3$): δ 14.00, 22.57, 25.91, 29.11, 29.23, 29.45, 29.54, 31.79, 67.92, 69.89, 92.22, 114.52, 114.68, 126.88, 127.59, 127.78, 128.58, 128.74, 132.02, 135.41, 159.11, 162.37, 183.89, 185.98. FABMS (m/z), calcd for M^+ 514.69, found 514.90. Anal. Calcd for $C_{34}H_{42}N_2O_4$: C, 79.34; H, 8.22. Found: C, 79.75; H, 8.34.

4.1.6. 5-[4-(4-Dodecyloxybenzyloxy)phenyl]-3-phenyl-1*H*-pyrazole (2; *n*=12). The synthetic procedures were similarly followed as above for the compound **1a** (n=16). White solid, yield 82%. ^{1}H NMR ($CDCl_3$): δ 0.88 (t, J=8.4 Hz, –CH_3, 3H), 1.24–1.80 (m, –CH_2, 20H), 3.94 (t, J=6.5 Hz, –OCH_2, 2H), 4.94 (s, –CH_2, 2H), 6.71 (s, –CNCH, 1H), 6.90 (dd, J=3.0, 8.7 Hz, –C_6H_4, 2H), 7.28 (d, J=6.1 Hz, –C_6H_4, 2H), 7.33 (s, –C_6H_5, 1H), 7.35 (d, J=6.1 Hz, –C_6H_4, 2H), 7.58 (d, J=8.7 Hz, –C_6H_4, 2H), 7.68 (dd, J=2.1 Hz, 7.7 Hz, –C_6H_5, 2H). ^{13}C NMR ($CDCl_3$): δ 13.92, 22.59, 26.03, 29.25, 29.30, 29.34, 29.59, 31.86, 68.26, 70.11, 99.55, 114.82, 115.45, 124.32, 125.66, 126.94, 128.02, 128.74, 128.85, 129.03, 131.79, 159.16, 159.23. FTIR (KBr): 3240, 2917, 2849, 1558, 1540, 1519, 1473, 1457, 1252, 1176, 1051, 1027, 1011, 968, 826, 796, 761 cm^{-1}. Anal. Calcd for $C_{34}H_{42}N_2O_2$: C, 79.96; H, 8.29; N, 5.49. Found: C, 79.88; H, 8.40; N, 5.54.

4.1.7. 4-Hexadecyloxyacetophenone[15d] (*n*=16). White solid, yield 93%. ^{1}H NMR ($CDCl_3$): δ 0.84 (t, J=6.1 Hz, –CH_3, 3H), 1.25–1.79 (m, –CH_2, 28H), 2.45 (s, –$COCH_3$, 3H), 3.94 (t, J=6.5 Hz, –OCH_2, 2H), 6.85 (d, J=6.8 Hz, –C_6H_4, 2H), 7.84 (d, J=6.8 Hz, –C_6H_4, 2H). ^{13}C NMR ($CDCl_3$): δ 13.96, 22.25, 25.74, 26.13, 27.80, 29.06, 29.18, 29.56, 31.66, 68.13, 113.78, 129.87, 130.47, 162.93, 196.54. FABMS (m/z), calcd for M^+ 560.57, found $(M+1)^+$ 561.40.

4.1.8. (4-Ferrocenylphenyl)methanol. This compound has been reported previously in the literatures.[5] A THF solution of ethyl 4-ferrocenylbenzoate (10.0 g, 0.027 mol) was added dropwise to a solution of $LiAlH_4$ (2.61 g, 0.07 mol) dissolved in 30 mL of THF. The mixture was stirred for 24 h at room temperature. The solution was carefully quenched with dilute hydrochloric acid (0.5 M) at 0 °C, and the solution was extracted with 100 mL of CH_2Cl_2. The deep red organic solutions were collected and dried over anhydrous $MgSO_4$. The solution was concentrated to give crude red solids. The product isolated as red crystals was obtained by recrystallization from CH_2Cl_2/MeOH. Yield 80%. ^{1}H NMR ($CDCl_3$): δ 4.02 (s, –C_5H_5, 5H), 4.31 (t, –C_5H_4, 2H), 4.63 (m, –CH_2, –C_5H_4, 4H), 7.26 (d, J=8.0 Hz, –C_6H_4, 2H), 7.45 (d, J=7.9 Hz, –C_6H_4, 2H). ^{13}C NMR ($CDCl_3$): δ 65.12, 66.35, 68.79, 69.45, 84.90, 126.01, 127.0, 138.22, 138.62.

4.1.9. 1-Chloromethyl-4-ferrocenylbenzene. (4-Ferrocenylphenyl)methanol (10.0 g, 0.003 mol) was completely dissolved in 200 mL of dried THF, and the solution was then carefully added to thionyl chloride (23.5 mL, 0.34 mol) at ice bath temperature. The solution was stirred for 4 h at room temperature. The excess of $SOCl_2$ was removed by vacuum in the hood. The viscous residue was washed with dried THF, and the solution was then concentrated by vacuum again. The process of wash-and-pump was repeatedly followed three times, and the product

isolated as powder was directly used for the next step without any other purification.

4.1.10. 4-(4-Ferrocenylbenzyloxy)benzoic acid methyl ester.[5] A mixture of methyl-4-hydroxyacetophenone (5.0 g, 0.035 mol), anhydrous K_2CO_3 (5.66 g, 0.039 mol), KI (catalytic amount), and 1-chloromethyl-4-ferrocenylbenzene (21.74 g, 0.07 mol) was dissolved in 250 mL of dried acetone under nitrogen atmosphere. The solution was refluxed for 48 h. The solution was cooled to room temperature and then filtered to remove solids by suction. The solution was first washed with aqueous brine solution and then extracted twice with CH_2Cl_2. The organic solution was combined and dried over anhydrous Na_2SO_4. The product was purified by flash chromatography with hexane/CH_2Cl_2 (2:1). Yellow crystals were isolated after recrystallization from CH_2Cl_2/CH_3OH. Yield 42%. ^{1}H NMR ($CDCl_3$): δ 3.87 (s, –OCH_3, 3H), 4.05 (s, –C_5H_5, 5H), 4.30 (t, J=1.8 Hz, –C_5H_4, 2H), 4.62 (t, J=1.8 Hz, –C_5H_4, 2H), 5.06 (s, –CH_2, 2H), 6.99 (d, J=6.9 Hz, –C_6H_4, 2H), 7.32 (d, J=8.2 Hz, –C_6H_4, 2H), 7.46 (d, J=6.5 Hz, –C_6H_4, 2H), 8.00 (d, J=6.8 Hz, –C_6H_4, 2H). ^{13}C NMR ($CDCl_3$): δ 51.75, 66.42, 69.00, 69.48, 69.93, 84.68, 114.30, 122.62, 126.19, 127.59, 131.47, 133.46, 139.35, 162.41, 166.71. Anal. Calcd for $C_{25}H_{22}O_3Fe$: C, 70.44; H, 5.20. Found: C, 70.58; H, 5.39.

4.1.11. 1-[4-(4-Ferrocenylbenzyloxy)phenyl]-3-(4-decyloxyphenyl)propane-1,3-dione (3b; *n*=10). The synthetic procedures were similarly followed as above for the compound. Deep red solid, yield 68%. ^{1}H NMR ($CDCl_3$): δ 0.88 (t, J=6.1 Hz, –CH_3, 3H), 1.33–1.85 (m, –CH_2, 16H), 4.00 (t, J=3.1 Hz, –OCH_2, 2H), 4.03 (s, –C_5H_5, 5H), 4.31 (t, J=1.8 Hz, –C_5H_4, 2H), 4.63 (t, J=1.9 Hz, –C_5H_4, 2H), 5.05 (s, –CH_2, 2H), 6.68 (s, –CCHCO, 1H), 6.93 (d, J=8.9 Hz, –C_6H_4, 2H), 7.04 (d, J=8.9 Hz, –C_6H_4, 2H), 7.35 (d, J=8.3 Hz, –C_6H_4, 2H), 7.48 (d, J=8.3 Hz, –C_6H_4, 2H), 7.64 (d, J=5.4 Hz, –C_6H_4, 4H), 17.12 (s, –OH, 1H). ^{13}C NMR ($CDCl_3$): δ 14.00, 22.55, 25.84, 29.00, 29.21, 29.42, 29.45, 31.78, 66.42, 68.12, 68.90, 69.48, 69.70, 84.67, 91.33, 114.25, 114.52, 126.61, 127.61, 127.71, 128.23, 128.93, 133.49, 139.37, 162.06, 162.53, 183.26, 184.61. FTIR (KBr): 3097, 2918, 2850, 1603, 1508, 1498, 1471, 1259, 1228, 1173, 1120, 1002, 841, 818, 784 cm^{-1}. FABMS (*m*/*z*), calcd for M^+ 670.27, found 670.47. Anal. Calcd for $C_{42}H_{46}O_4Fe$: C, 75.22; H, 6.91. Found: C, 75.54; H, 7.02.

4.1.12. 3-[4-(4-Ferrocenylbenzyloxy)phenyl]-5-(4-decyloxyphenyl)-1*H*-pyrazole (1b, *n*=10). The synthetic procedures were similarly followed as above for the compound. Yellow-orange solid, yield 84%. ^{1}H NMR ($CDCl_3$): δ 0.93 (t, J=6.3 Hz, –CH_3, 3H), 1.33–1.85 (m, –CH_2, 16H), 4.03 (t, J=2.6 Hz, –OCH_2, 2H), 4.08 (s, –C_5H_5, 5H), 4.35 (t, J=2.0 Hz, –C_5H_4, 2H), 4.68 (t, J=1.9 Hz, –C_5H_4, 2H), 5.10 (s, –CH_2, 2H), 6.71 (s, –CCHCO, 1H), 6.98 (d, J=8.2 Hz, –C_6H_4, 2H), 7.06 (d, J=8.2 Hz, –C_6H_4, 2H), 7.39 (d, J=7.9 Hz, –C_6H_4, 2H), 7.53 (d, –C_6H_4, 2H), 7.67 (dd, J=2.1, 7.2 Hz, –C_6H_4, 4H). ^{13}C NMR ($CDCl_3$): δ 13.99, 22.62, 25.06, 29.27, 29.32, 29.40, 29.53, 31.87, 66.56, 68.23, 68.95, 69.59, 70.18, 85.08, 99.02, 114.94, 115.31, 124.07, 124.70, 126.29, 126.92, 126.98, 127.63, 134.42, 139.24, 159.02, 159.35. FABMS (*m*/*z*), calcd for M^+ 666.67, found 666.85. FTIR (KBr): 3244, 3072, 3034, 2934, 2862, 1616, 1505, 1457, 1448, 1246, 1173, 1105, 1038, 968, 834, 822, 791 cm^{-1}. Anal. Calcd for $C_{42}H_{46}N_2O_2Fe$: C, 75.67; H, 6.95; N, 4.20. Found: C, 75.74; H, 6.85; N, 3.90.

Acknowledgements

We thank the National Science Council of Taiwan, ROC, for funding (NSC-92-2113-M- 008-003) in generous support of this work.

Supplementary data

Supplementary data associated with this article can be found in the online version, at doi:10.1016/j.tet.2006.06.028.

References and notes

1. (a) Togni, A.; Hayashi, T. *Ferrocenes*; VCH: Weinheim, 1995; (b) Van Staveren, D. R.; Metzler-Nolte, N. *Chem. Rev.* **2004**, *104*, 5931–5986; (c) Bruce, D. R.; O'Hare, D. *Inorganic Materials*, 2nd ed.; Wiley: New York, NY, 1996.
2. Serrano, J. L. *Metallomesogens: Synthesis, Properties, and Applications*; VCH: Weinheim, 1996.
3. Malthête, J.; Billard, J. *Mol. Cryst. Liq. Cryst.* **1976**, *34*, 117–134.
4. (a) Cook, M. J.; Cooke, G.; Jafari-Fini, A. *Chem. Commun.* **1996**, 1925–1926; (b) Andreu, R.; Garin, J.; Orduna, J.; Barbera, J.; Serrano, J. L.; Sierra, T.; Salle, M.; Gorgues, A. *Tetrahedron* **1998**, *54*, 3895–3912; (c) Bissell, R. A.; Boden, N.; Bushby, R. J.; Fishwick, C. W. G.; Holland, E.; Movaghar, B.; Ungar, G. *Chem. Commun.* **1998**, 113–114; (d) Deschenaux, R.; Marendaz, J. L. *J. Chem. Soc., Chem. Commun.* **1991**, 909–910; (e) Imrie, C.; Loubser, C. *J. Chem. Soc., Chem. Commun.* **1994**, 2159–2160.
5. (a) Imrie, C.; Engelbrecht, P.; Loubser, C.; McCleland, C. W. *Appl. Organomet. Chem.* **2001**, *15*, 1–15; (b) Imrie, C.; Loubser, C.; Engelbrecht, P.; McCleland, C. W.; Zheng, Y. *J. Organomet. Chem.* **2003**, *665*, 48–64; (c) Imrie, C.; Engebrecht, P.; Loubser, C.; Mcleand, C. W.; Nyamori, V. O.; Bogardi, R.; Levendis, D. C.; Tolom, N.; van Rooyen, J.; William, N. *J. Organomet. Chem.* **2002**, *645*, 65–81.
6. (a) Loubser, C.; Imrie, C. *J. Chem. Soc., Perkin Trans. 2* **1997**, 399–410; (b) Loubser, C.; Imrie, C.; van Rooyen, P. H. *Adv. Mater.* **1993**, *5*, 45–47; (c) Seshadri, T.; Haupt, H. J. *J. Mater. Chem.* **1998**, *8*, 1345–1350.
7. Seshadri, T.; Haupt, H. J. *Chem. Commun.* **1998**, 735–736.
8. (a) Campidelli, S.; Vázquez, E.; Milic, D.; Prato, M.; Barberá, J.; Guldi, D. M.; Marcaccio, M.; Paolucci, D.; Paolucci, F.; Deschenaux, R. *J. Mater. Chem.* **2004**, *14*, 1266–1272; (b) Even, M.; Heinrich, B.; Guillon, D.; Guldi, D. M.; Prato, M.; Deschenaux, R. *Chem.—Eur. J.* **2001**, *7*, 2595–2604; (c) Deschenaux, R.; Even, M.; Guillon, D. *Chem. Commun.* **1998**, 537–538.
9. (a) Cook, M. J.; Cooke, G.; Jafan-Fini, A. *J. Chem. Soc., Chem. Commun.* **1995**, 1715–1716; (b) Deschenaux, R.; Mounnet, F.; Serrano, J. L.; Turpin, F. *Helv. Chim. Acta* **1998**, *81*, 2072–2077; (c) Seo, J. S.; Yoo, Y. S.; Choi, M. G. *J. Mater. Chem.* **2001**, *11*, 1332–1338.
10. Barberá, J. J.; Cativiela, C.; Serrano, J. L.; Zurbano, M. M. *Liq. Cryst.* **1992**, *11*, 887–897.
11. Lin, H. D.; Lai, C. K. *J. Chem. Soc., Dalton Trans.* **2001**, 2383–2387.

12. (a) Murray, H. H.; Raptis, R. G.; Fackler, J. P. *Inorg. Chem.* **1988**, *27*, 26–33; (b) Bovio, B.; Bonati, F.; Banditelli, G. *Inorg. Chim. Acta* **1984**, *87*, 25–33; (c) Minghetti, G.; Banditelli, G.; Bonati, F. *Inorg. Chem.* **1979**, *18*, 658–663.
13. (a) Barberá, J.; Elduque, A.; Giménez, R.; Oro, L. A.; Serrano, J. L. *Angew. Chem., Int. Ed.* **1996**, *35*, 2832–2835; (b) Barberá, J.; Giménez, R.; Serrano, J. L. *Chem. Mater.* **2000**, *12*, 481–489; (c) Barberá, J.; Elduque, A.; Giménez, R.; Lahoz, F.; López, J. A.; Oro, L. A.; Serrano, J. L. *Inorg. Chem.* **1998**, *37*, 2960–2967.
14. Kim, S. J.; Kang, S. H.; Park, K. M.; Kim, H.; Zin, W. C.; Choi, M. G.; Kim, K. *Chem. Mater.* **1998**, *10*, 1889–1893.
15. (a) Lai, C. K.; Ke, Y. C.; Su, J. C.; Li, W. R. *Liq. Cryst.* **2002**, *29*, 915–920; (b) Li, W. R.; Kao, K. C.; Yo, Y. C.; Lai, C. K. *Helv. Chim. Acta* **1999**, *82*, 1400–1407; (c) Lai, C. K.; Lu, M. Y.; Lin, F. J. *Liq. Cryst.* **1997**, *23*, 313–315; (d) Yang, C. D.; Pang, Y. S.; Lai, C. K. *Liq. Cryst.* **2001**, *28*, 191–195.
16. (Ina) du Plessis, W. C.; Davis, W. L.; Cronje, S. J.; Swarts, J. C. *Inorg. Chim. Acta* **2001**, *314*, 97–104.